LASER INTERFEROMETER GRAVITATIONAL WAVE OBSERVATORY
- LIGO -
CALIFORNIA INSTITUTE OF TECHNOLOGY
MASSACHUSETTS INSTITUTE OF TECHNOLOGY

Technical Note	**LIGO-TXXXXXXX–vX**	2024/06/14

Visible Light Fabry-Perot Cavity

Peter Carney, Dr. Jonathan Richardson

California Institute of Technology
LIGO Project, MS 18-34
Pasadena, CA 91125
Phone (626) 395-2129
Fax (626) 304-9834
E-mail: info@ligo.caltech.edu

Massachusetts Institute of Technology
LIGO Project, Room NW22-295
Cambridge, MA 02139
Phone (617) 253-4824
Fax (617) 253-7014
E-mail: info@ligo.mit.edu

LIGO Hanford Observatory
Route 10, Mile Marker 2
Richland, WA 99352
Phone (509) 372-8106
Fax (509) 372-8137
E-mail: info@ligo.caltech.edu

LIGO Livingston Observatory
19100 LIGO Lane
Livingston, LA 70754
Phone (225) 686-3100
Fax (225) 686-7189
E-mail: info@ligo.caltech.edu

http://www.ligo.caltech.edu/

Abstract

The LIGO Lab at UC Riverside develops a table-top scale Fabry-Perot optical cavity with 532nm visible light. We design and commission a con-focal cavity with mirrors of 0.4m ROC. The cavity is 0.55m in length and has a Finesse of 207. The visible light optical cavity also incorporates an analog Pound-Drever-Hall locking system, actuating on the ETM position.

Contents

1 Introduction

In 1916, Albert Einstein's theory of General Relativity predicted the existence of propagating waves in the metric of spacetime. These propagating waves in spacetime originate from accelerating massive objects such as binary black holes and neutron stars, and they have come to be known as gravitational-waves. Gravitational-waves have extremely small strain, which is the distance and object is stretched or compressed relative to the original length of the object $h = \Delta L/L$. Because of this, Einstein himself never thought these waves could be detected. However, with the creation of the Laser Interferometer Gravitational-Wave Observatory (LIGO), physicists were able to detect the first gravitational-wave in 2017 from a Binary black hole merger event.

In principle, LIGO operates as a Michelson interferometer (as seen in Figure 1.1), in which a laser of 1064nm wavelength is split into two perpendicular directions of equal length. In the nominal condition, light will travel down each direction, and return to the beam splitter in which the electromagnetic waves will destructively interfere. The destructive interference leads to no light signal being seen in the readout port. As a strong gravitational wave propagates through the detector, the elongation of the interferometer in one direction (or arm) will result in a contraction in the perpendicular direction. As light travels down each direction, the difference in arm length will result in a non-perfect destructive interference, and the difference in the phases of the light in each direction will allow detection of the gravitational wave in the readout port.

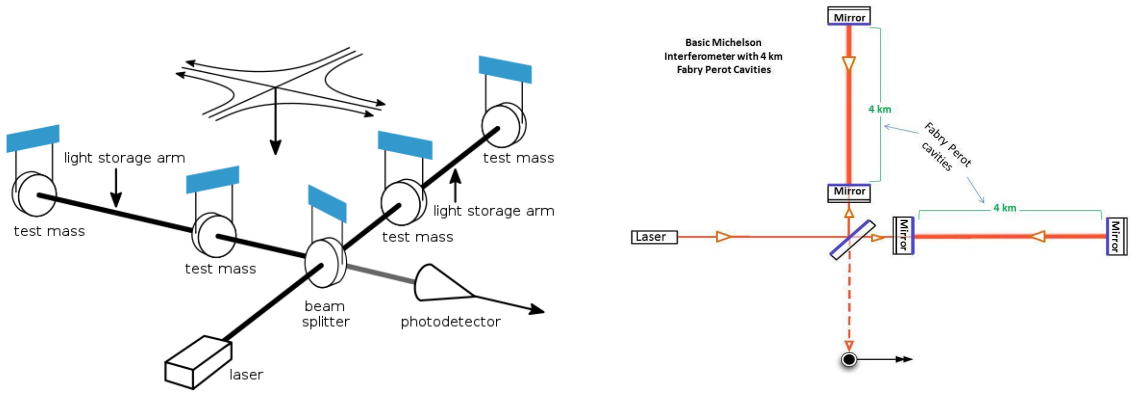

Figure 1.1: *Left: The principle of the Michelson interferometer. The gravitational wave can be seen above propagating down into the plane of the detector. As one arm increases in length, the other will decrease, causing decoherence in the propagating waves. Right: The design of the Fabry-Perot cavities within the detector. As the photon enters the cavity, it will propagate back and forth approximately 300 times before exiting back into the beamsplitter and then the readout port.*

Considering that $h = 10^{-21}$, the LIGO interferometer needs to be incredibly sensitive. LIGO has implemented many clever upgrades in order to significantly increase their sensitivity. While all of the upgrades are seen in the right of Figure 1, one of the most important features is the Fabry-Perot optical cavity that exists within each LIGO arm. By placing a

mirror with a slightly curved surface immediately after the beam splitter, LIGO creates a condition in each arm in which the photon will propagate back and forth roughly 300 times before exiting the cavity. This results in two significant affects. First, the build-up of power will reduce error in the phase of the electromagnetic wave. Secondly, the photon will effectively travel a farther distance before exiting the cavity and making it to the readout port, which will increase the relative strain, $h = \Delta L/L$.

The Fabry-Perot optical cavity is a highly important feature in LIGO that significantly contributes to its sensitivity. This technical note focuses on the physics, engineering and design of a Fabry-Perot cavity on the tabletop scale. Our tabletop cavity uses a 532nm wavelength laser, allowing users to more easily observe / demonstrate the cavity's properties. This cavity uses a 1mW laser, which will not only be easily visible, but allow safe interaction with users and observers. The full schematic of the visible light optical cavity is shown in Figure 1.2 below, which will be carefully explained in this technical note.

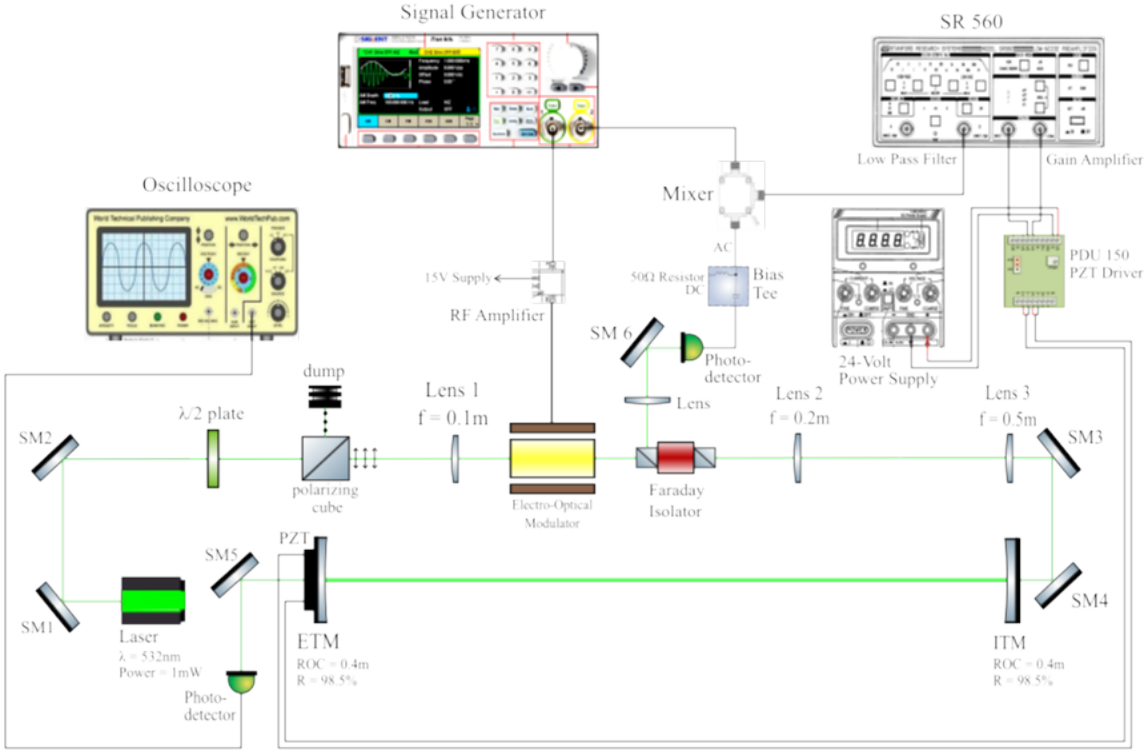

Figure 1.2: *The full design of the visible light optical cavity. Prior to the cavity is a chain of launch optics to prepare the beam to enter the cavity. The cavity is stabilized by a feedback control system. These components will all be explained in the following sections*

In all optical cavities, a power resonance is formed when the length of the cavity is a half integer multiple of the wavelength of the light, or when the condition $L = \frac{n\lambda}{2}$ is true, in which $n = 1, 2, 3, ...$ Considering the natural drift and fluctuation of the laser frequency, we need

to actively control either the laser frequency or the cavity length in order to keep the cavity locked to its resonance condition. This tabletop cavity will use a technique known as the Pound Drever Hall (PDH) method in order to actuate on the end mirror's (ETM) position. The electronic configuration of the PDH feedback controll loop is seen in Figure 1.2 More information on the locking scheme and the PDH is given in the following sections (and in ref()).

This technical note first details the computer modeling that goes into defining the cavity and laser beam's target parameters. The paper will then give a summary of the acquired laser beam's characteristics. Thereafter, the technical note will detail other cavity components acquired, the procedure for assembling and commissioning the cavity, and software needed for the work.

2 FINESSE, Python, and Matlab Modeling

Before the cavity can be constructed, there are multiple components of the cavity that must be modeled, and many cavity parameters that must be pre-determined. A significant portion of this work is done in a software program called FINESSE. This program is designed to simulate a wide variety of optical set-ups and designs. FINESSE has many built-in functions that can calculate parameters about the laser, PDH lock, and other aspects of interferometery. FINESSE can work in tandem with Python. It acts as a parsed script within the python code that is read out by specific python commands. However, much of FINESSE's output and functions can be manipulated in python to allow a wide variety of functions depending on the user's desires.

Throughout this technical note, many of the plots and simulated data are generated through FINESSE. The python script itself is run through a Jupyter notebook. For detailed documentation about how to install and use FINESSE, visit ref[4] and ref[5]. To install and use Jupyter notebooks, please visit ref[5]. Much of this information is also in the Git repository listed in the abstract.

2.1 Cavity Eigenmode

In all optical cavities, high resonance is achieved by matching the laser beam to what is known as the cavity's eigenmode. In order to find what the cavity eigenmode is, we must first be more detailed in how we model our laser. We must take into account it's finite spatial features in the transverse directions. To model a finite beam of propagating light, we confine our electromagnetic wave to a finite space in the transverse directions. Most of the following information is gathered from Ref[1] and [2].

In order to confine the laser beam in the radial direction and satisfy the wave equation, the beam profile becomes fundamentally Gaussian (higher order modes HOM can exist as solutions to the wave equation, and can arise in situations where the electromagnetic field is perturbed). For now, we will only concern ourselves with the fundamental Gaussian mode.(More information can be found in [1]

As the Gaussian beam propagates, the beam size varies. A side profile of an ideal Gaussian beam is shown in Figure 2.1. Based off of this propagation style, we can define various parameters of our Gaussian beam. ω_0 is the width of the beam at it's minimum size, otherwise known as the beam waist. We then define z_0 as the position of the beam waist along the z-axis.

z_R is the *Rayleigh range* of the beam, which is z position at which the beam enters the far field. The Rayleigh range is defined as:

$$z_R = \frac{\pi \omega_0^2}{\lambda} \tag{2.1}$$

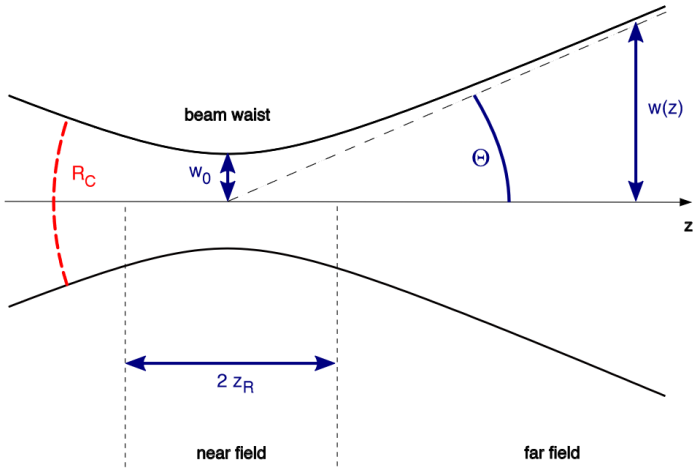

Figure 2.1: *From Interferometer Techniques for Gravitational Wave Detection: Figure 9.5: Gaussian beam profile along z: this cross section along the x-z-plane illustrates how the beam size $\omega(z)$ of the Gaussian beam changes along the optical axis.*

$\omega(z)$ is the width of the beam as position z. With knowledge of the Rayleigh range, it can be defined as

$$\omega(z) = \omega_0 \sqrt{1 + \left(\frac{z - z_0}{z_R}\right)^2} \tag{2.2}$$

In Figure 2.1, Θ is the *diffraction angle*, which is the angle between the z-axis and the beam width, $\omega(z)$. Lastly, we define our wavefront radius of curvature, R_C

$$R_C = z - z_0 + \frac{(z_R)^2}{z - z_0} \tag{2.3}$$

With knowledge of all of these parameters, it becomes possible to compactly model how the Gaussian modes interact with optical components by defining the *the Gaussian beam parameter, q*. This parameter comes with both a real and imaginary component, and can be determined through equations (2.4) and (2.5).

$$\frac{1}{q(z)} = \frac{1}{R_C} - i\frac{\lambda}{\pi\omega^2(z)} \tag{2.4}$$

$$q(z) = iz_R + (z - z_0) \tag{2.5}$$

For our analysis, it becomes useful to define the q parameter in terms of equation (2.6).

$$\omega^2(z) = \frac{\lambda}{\pi}\frac{|q|^2}{\mathrm{Im(q)}} \tag{2.6}$$

As the q parameter interacts with optical components, it becomes transformed. Each transformation by an optical component is modeled by a 2x2 matrix associated with that optical

component. Since our laser resonates within two mirrors and free space within those two mirrors, we define two transformations:

Reflection at a Curved Surface

$$M = \begin{pmatrix} 1 & 0 \\ -\frac{2n_1}{R_C} & 1 \end{pmatrix}$$

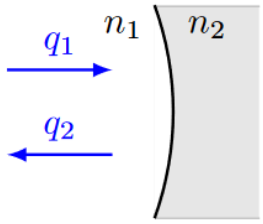

Transmission through a free space:

$$M = \begin{pmatrix} 1 & \frac{L}{n} \\ 0 & 1 \end{pmatrix}$$

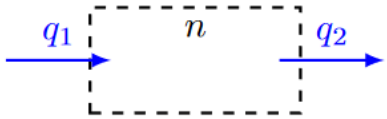

As the beam propagates through the cavity, it's round trip will resemble Figure 2.2.

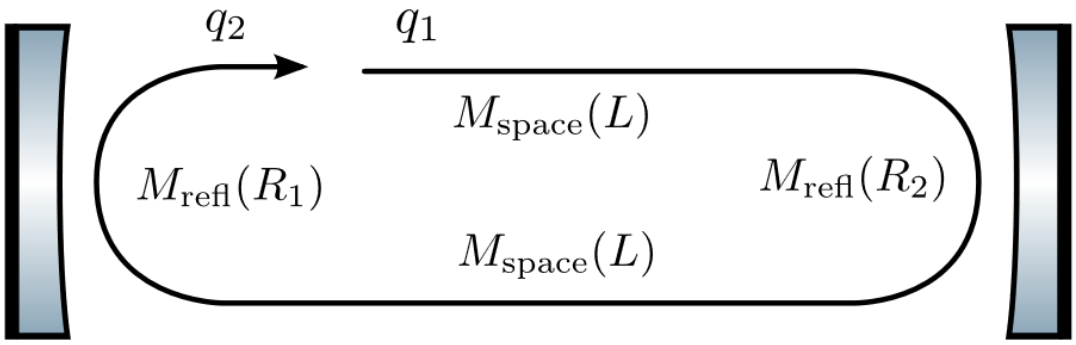

Figure 2.2: *From Interferometer Techniques for Gravitational Wave Detection: Figure 9.18: Cavity round trip ABCD matrices for a 2-mirror cavity*

Successive transformations through multiple optical components is represented by multiplying the matrices together. The total transformation for a round trip of a 2 mirror cavity will be:

$$\begin{pmatrix} A & B \\ C & D \end{pmatrix} = \begin{pmatrix} 1 & \frac{L}{n} \\ 0 & 1 \end{pmatrix} \begin{pmatrix} 1 & 0 \\ -\frac{2n}{R_2} & 1 \end{pmatrix} \begin{pmatrix} 1 & \frac{L}{n} \\ 0 & 1 \end{pmatrix} \begin{pmatrix} 1 & 0 \\ -\frac{2n}{R_1} & 1 \end{pmatrix} \tag{2.7}$$

Where n is the index of refraction (which for the tabletop cavity is air, so n = 1), and R_1 and R_2 are the radii of curvature of mirrors 1 and 2 respectively. Finally, our transformation

of the q parameter becomes:

$$q_2 = \frac{Aq_1 + B}{Cq_1 + D} \tag{2.8}$$

After a round trip, when $q_1 = q_2$, the Gaussian beam's spatial profile has been recreated. This condition becomes known as the cavity's eigenmode. We can find the cavity eigenmode, $q_{cav} = q_1 = q_2$ by solving the equation:

$$Cq_{cav}^2 + (D - A)q_{cav} - B = 0. \tag{2.9}$$

which is a simple quadratic equation. For our tabletop visible light Fabry-Perot cavity, this analysis has been done using a simple Python code. In our analysis, the radii of curvature for both the ITM and ETM are

$$R_1 = R_2 = 400mm$$

meaning that we have a con-focal cavity. The distance between the two mirrors is $L = 0.55m$. With these conditions, the q parameter and beam width at the ITM are:

$$q = 0.275 + i0.185$$

$$\omega(z) = 0.3169mm$$

This analysis was also cross-checked with FINESSE software. The cavity conditions were recreated in the FINESSE syntax using the same radii of curvature and cavity length. The longitudinal beam profile and data sheet have been recreated and are shown in Figure 2.3 below.

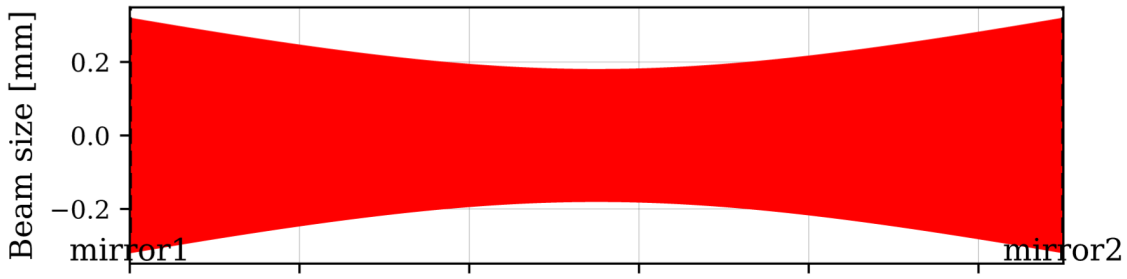

	z	w0	zr	w	RoC	Acc. Gouy	q
Laser.p1.o	0 m	177.19 um	185.4 mm	316.97 um	-400 mm	0°	-0.275 + 0.185j
mirror1.p1.i	0 m	177.19 um	185.4 mm	316.97 um	-400 mm	0°	-0.275 + 0.185j
mirror1.p2.o	0 m	177.19 um	185.4 mm	316.97 um	-400 mm	0°	-0.275 + 0.185j
mirror2.p1.i	550 mm	177.19 um	185.4 mm	316.97 um	400 mm	112.02°	0.275 + 0.185j

Figure 2.3: *Top: Side profile of Visible Light Cavity laser. Bottom. Visible Light Cavity Eigenmode Data*

2.2 Cavity finesse

From the introduction, we remember that light transmits through the cavity when the length of the cavity is a half integer multiple of the wavelength of the light, or when $L = \frac{n\lambda}{2}$. This means that as we sweep through a large enough range of laser frequencies, the cavity will go through repeated conditions of resonance. This will produce a power vs. frequency plot as seen in Figure 2.4.

Since the laser frequency is $\nu = c/\lambda$, we can write: $L = \frac{nc}{2\nu}$. The Free Spectral Range is defined as the frequency difference between two successive frequencies allowing for a resonance condition. Hence, if we take the difference between these equations for n=1 and n=2, we find that.

$$\Delta\nu_{FSR} = \frac{c}{2L} \tag{2.10}$$

Essentially, the FSR is the frequency difference between successive peaks. The width of the peaks themselves is known as the Finesse of the cavity, and it is directly dependent on the reflectivities of the mirror surfaces. The Finesse can be directly calculated with the equation below. (Ref[6])

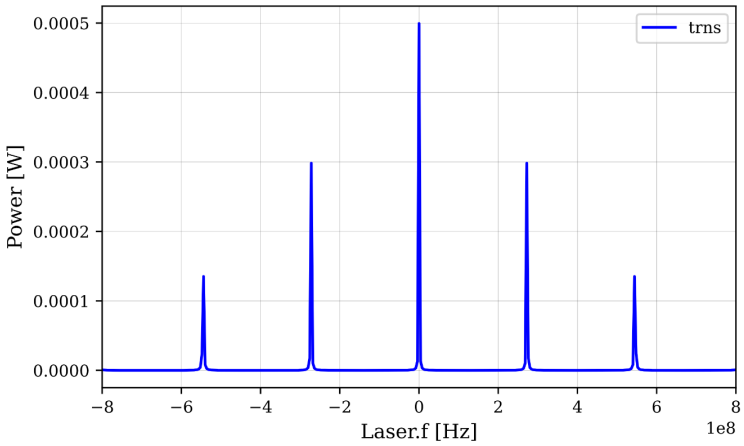

Figure 2.4: *FINESSE generated plot of the frequency spectrum. The curve represents transmitted power through the cavity. Our initial laser power is P = 0.5mW. The finesse is F = 207.86. The FSR = 272.54MHz*

$$F = \frac{\pi}{\sin\left(\frac{1-R_1R_2}{2\sqrt{R_1R_2}}\right)} \tag{2.11}$$

Here, R_1 and R_2 are the reflectivity of Mirrors' 1 and 2 curved surfaces respectively. Given this relation, we first determined what we wanted our finesse to be. Then, based off our desired range of finesse values, we choose what reflectivity we want our mirror coatings to have. The higher the finesse, the more power that is able to resonate within the cavity, yet

the narrower the peak is, and thus the harder it is to keep on resonance. The optimum value was determined to be a finesse of approximately 200. With this finesse, we determined that the reflectivity of each mirror surface be 98.5% (meaning 3% round-trip loss). These values were determined by using the python-generated heat map shown below.

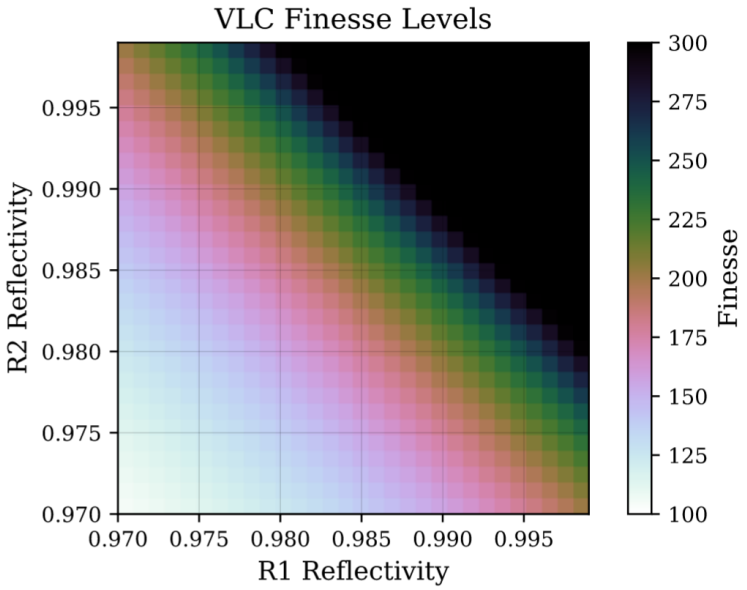

Figure 2.5: *Python-generated heat map of the Finesse as functions of each of the mirror's reflectivities. The optimal position was found at 98.5% for both mirrors.*

2.3 Mode matching telescope

Now that the cavity eigenmode is modeled, it becomes necessary to design a combination of lenses to transform the laser's original q-parameter and beam width to match the input q-parameter required for the cavity. This combination of lenses will be known as our mode matching telescope.

The optical set up will incorporate a 0.1m focal length lens prior to the electro-optical modulator (EOM). This is done in order to focus the beam fully into the EOM and Faraday Isolator ports. The lens creates a beam waist of 0.066mm at which we define our z = 0 position. A diagram for the mode matching set up is shown in Figure 2.6.

There are two separate computer programs used to design the mode matching telescope: one is in FINESSE/Python, and the other is a script in Matlab called A La Mode. Both of these scripts will be used to identify the target q parameter for the VLC, and they will serve to cross check each other.

The FINESSE/Python program uses the relative distances between the lenses and ITM in order to find the best possible mode matching. The FINESSE model defines the beam waist

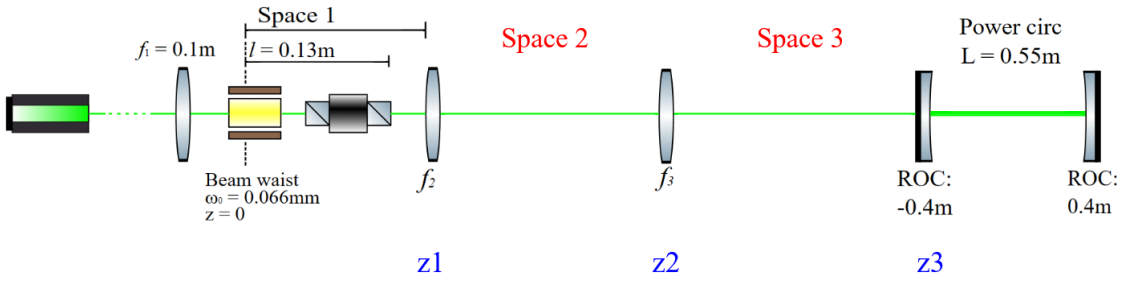

Figure 2.6: *Mode matching conceptual design for modeling in FINESSE and Matlab. Red text are parameters to be used in FINESSE. Blue text are parameters to be used in Matlab.*

to be at z=0. There are two lenses of pre-defined focal lengths prior to the VLC. The model includes a photo-detector on the output side of the ETM in order to measure the power when the cavity reaches as resonance condition. When the mode matching telescope is optimized, the pd will read maximum power. Then, Python is used to tune the distances between the lenses in order to find the optimum distance relation. By having two adjustable parameters to measure the output power, the heat map in Figure 2.7 is created showing the range of spacing between the lenses that results in best mode matching.

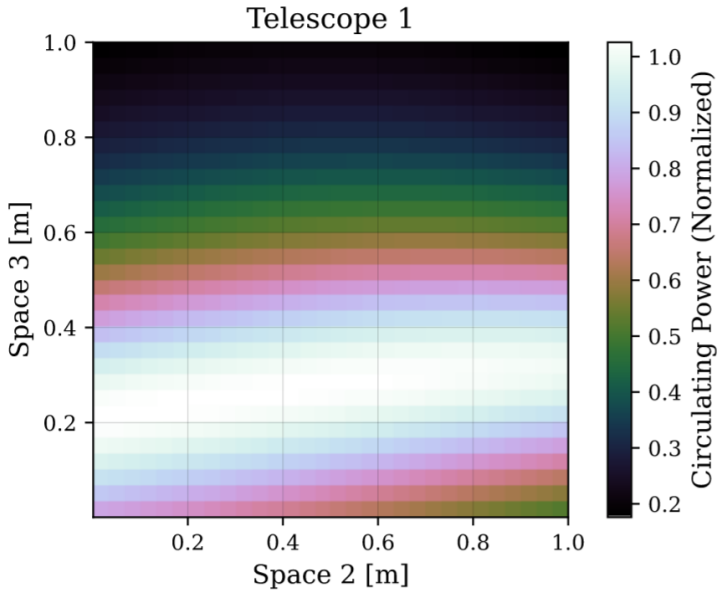

Figure 2.7: *Heat map to indicate best distances for mode matching. The output power is normalized to the maximum power possible.*

The heat map is efficient to analyze for several reasons. First, it gives a variety of relative spacing between lenses to choose from in designing the mode matching telescope. The other reason is that it shows the error tolerance to change in position. Since Figure 2.7 has a large area creating resonance conditions, we are less likely to be susceptible to error in our positioning when implementing this set-up on the optical table.

Now that we identified a good range of spacings in FINESSE, A La Mode is then used to pin-point the exact positions of the lenses to give us perfect mode matching. Instead of using the spacing between the lenses, A La Mode uses their position along the z-axis (or the beam axis), and does the ABCD matrix calculation to find the best positions to find the desired q-parameter. The code models a combination of 2 lenses, and a end position. The script is given an initial q-parameter. For our set-up in the VLC, the initial q is $q_{initial} = 0 + 0.0257i$. The script is then given a target q, which is $q_{final} = 0.275 + 0.1854i$. The user then inputs the maximum distance of the set of mode matching lenses, and the program cycles through many combinations of lens positions and focal lengths to give the best mode matching.

Since the FINESSE code gives us a good initial range to look in, the range of options to look through in A La Mode were narrowed down significantly. The final mode matching telescope parameters are shown in Table 1 below and the beam width and the gouy phase profile are shown in Figure 2.8 below.

Component	z-position (m)	focal length (m)
Lens 1	z = -0.1	f = 0.1
Lens 2	z = 0.1898	f = 0.2
Lens 3	z = 0.3284	f = 0.5
ITM	z = 0.5497	ROC = -0.4m

Table 1: Mode Matching Telescope Parameters. Note that lens 1 was already place prior to doing the mode matching analysis, since we used the beamwaist to define our z=0 point.

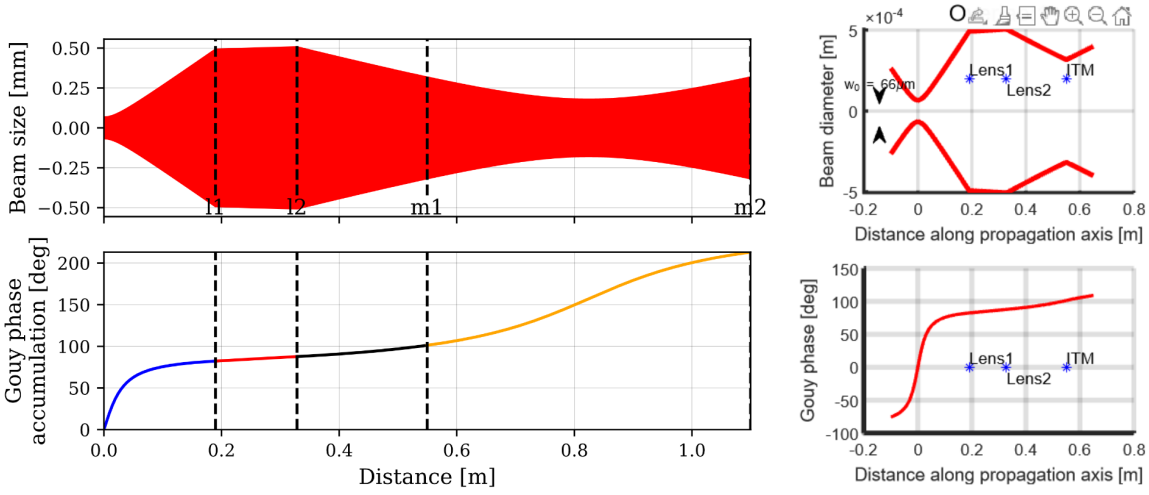

Figure 2.8: *Beam and gouy phase profile from FINESSE Output (Left) and A La Mode Output (Right).*

2.4 PDH Locking Scheme

It is assured that the laser frequency naturally drifts / fluctuates over time. In order to keep the visible light cavity locked onto resonance, we utilize a powerful technique known as the Pound-Drever-Hall (PDH) method. The PDH lock can be done by acting on the laser frequency to keep it constant or by acting on the cavity length to match the laser frequency change. For this visible light cavity, we actuate on the end mirror (ETM), thus varying the cavity length and keep it matched to resonance. This section details the principle behind the PDH method, and how we model it for the visible light cavity.

When the cavity is on resonance, the build up of power in the cavity allows a small percentage of the light to transmit through the ETM and first mirror (ITM). This intensity is measured via a photo-detector to determine if the cavity is on resonance. If the frequency deviates from being a half-integer multiple of the cavity length, then we no longer receive any transmitted light through the cavity. However, this won't work for doing a cavity lock, because if there is a decrease in the transmission intensity, we are not able to tell if it is a fluctuation in the frequency or the laser's intensity itself.

An easy way to distinguish between intensity fluctuations and frequency fluctuations is to measure the portion of the beam that gets reflected from the ITM prior to entering the cavity. No matter what the intensity is, as long as the frequency stays at a half integer multiple of the cavity length, the light that leaks out of the cavity through the ITM is 180 degrees out of phase from the promptly reflected beam and they destructively interfere, causing no light intensity at all (assuming we have a perfectly Gaussian laser beam that is well mode-matched). Upon frequency fluctuations, we see a reflected intensity, which is modeled in Figure 2.9

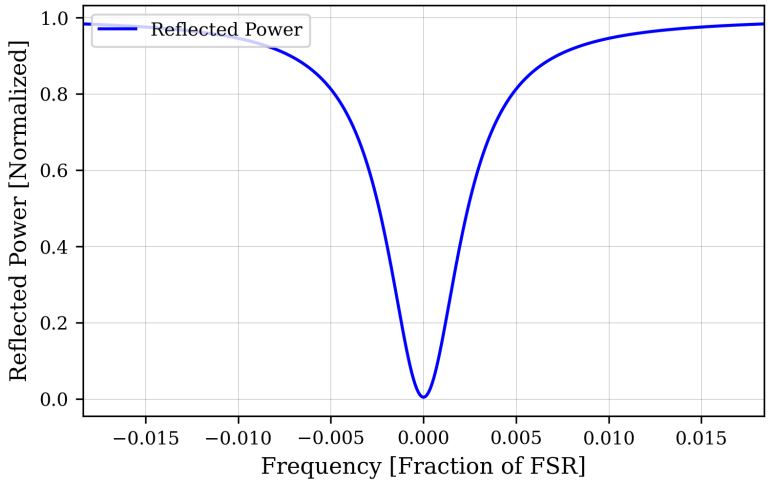

Figure 2.9: *FINESSE simulation of the promptly reflected beam from the ITM. The program simulates a photo-detector placed prior to the ITM. The frequency is changed +/- 5MHz and shown as a fraction of the cavity's FSR*

However, even this is difficult to correct because the shift in frequency is symmetric about resonance. If the frequency shifts, we are unable to determine which direction to move the ETM. Therefore we take the derivative of this signal to determine which way to drive ETM. If the frequency is above resonance (meaning wavelength decreases), then our derivative of the intensity curve is positive, and we decrease the cavity length to accommodate. If the frequency is below resonance (meaning the wavelength increases) then we have a derivative that is negative and we increase the length of our cavity. Taking the derivative of this error curve is not hard to do and it is the principle of the PDH method.

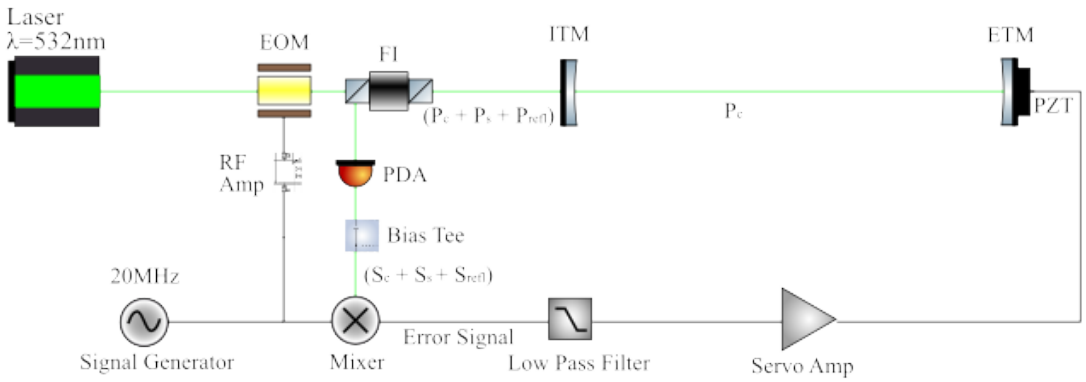

Figure 2.10: *Simplified PDH Locking Schematic. P_c is the carrier power, P_{refl} is the promptly reflected beam from the ITM, and P_s is the collective power from the two sidebands.*

In order to differentiate the reflected signal, we modulate the laser frequency a little bit and observe how the reflected beam responds. This is done with the set up shown in Figure 2.10 for our visible light cavity. The beam first enters an Electro-Optical Modulator (EOM). The EOM is being sent a 20MHz AC voltage signal (which is amplified by an Radio Frequency Amplifier). Upon being driven by this signal, the EOM takes a percentage of the beam and shift it's frequency Ω = 20MHz higher and Ω =20MHz lower. This concept is shown in Figure 2.11

The original wave is denoted as the carrier, and the modulated waves are the sidebands. The amount of power from the carrier that gets put into the sidebands is known as the modulation depth. It is ideal for the modulation depth to be << 1, because we want the vast majority of power to couple into the cavity to build resonance. Hence for our cavity, our modulation depth will be modeled at 0.1. In practice, the modulation depth will be set by the amount of voltage supplied to the EOM.

The reason we modulate at +/- 20MHz is because for our cavity specifically, we desire to have the sidebands placed well outside of the resonance peak. This causes the sidebands to not enter the cavity and only interfere with the reflected beam. It is possible to modulate at

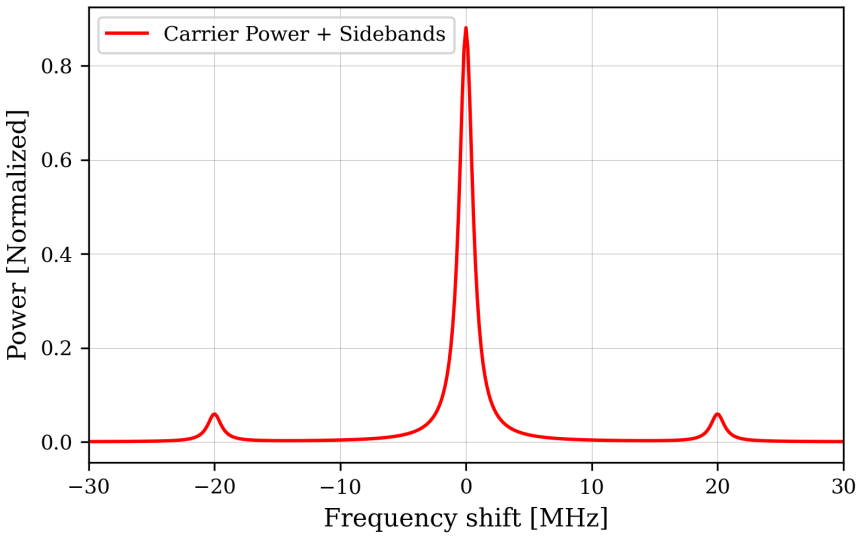

Figure 2.11: *Carrier power with sidebands shifted +/- 20MHz. Modulation depth is at 0.5 to make it easy to see the concept. In reality our modulation depth will be 0.1*

a low enough frequency in which the sidebands are within the resonance peak. This concept is qualitatively and quantitatively described in Ref[3].

Since the sidebands do not enter the cavity, they only interfere with the reflected beam which only appears if there is a frequency fluctuation. Upon a frequency fluctuation, the reflected beam and sidebands interfere. Since these fields are only slightly offset in frequency, they produce a beat note, which ultimately allows us to differentiate the between an increase or decrease in carrier frequency. This beat note propagtes back through the Faraday isolator and gets deflected to the photo-detector.

The photo-detector converts this signal into a voltage containing the carrier and beat note signal. Considering that our cavity is predicted to have power from higher order modes (section 3.1), we anticipate having a significant portion of the laser's power to be rejected from the cavity, which creates a signal that is significantly offset from zero, and thus creates a DC offset. In order to mitigate this we place a DC bias tee prior to the mixer, which allows the AC signal (which contains the beat note and other signals) to pass and dumps the DC offset. Considering that we have such short distance wires connecting everything, we do not worry about having a delay in phase of these signals, and thus do not include a phase shifter.

The signals from the cavity and signal generator are then sent into a mixer. The output of the mixer can be thought of as a product of all its inputs. This output is the error signal. The mathematics behind the fields that the mixer multiplies together is shown in Ref[3]. Since our cavity will be modulating at high frequency, our error signal will be given by equation (2.12) below.

$$\epsilon = 2\sqrt{P_c P_s}\mathrm{Im}\{F(\omega)F^*(\omega+\Omega) - F(\omega)F^*(\omega-\Omega)\} \quad (2.12)$$

Which is inherently imaginary. Here, $F(\omega)$ is the ratio of reflected power to carrier power. On resonance, since the reflected power is ideally 0, then $F(\omega)$ when ω is at its target frequency. The ratio is given by:

$$F(\omega) = \frac{E_{refl}}{E_{inc}} = \frac{r\left(e^{\frac{i\omega}{\Delta\nu_{FSR}}} - 1\right)}{1 - r^2\left(e^{\frac{i\omega}{\Delta\nu_{FSR}}}\right)} \tag{2.13}$$

Here, r is the amplitude of the reflection coefficient, $\Delta\nu_{FSR}$ is the Free spectral range, and ω is the angular frequency of our electric field. Given equation (2.13) we can take the amplitude squared $|F(\omega)|^2$ to find our total intensity. For the parameters of our visible light optical cavity, this is shown in Figure 2.12 below. Note that below our signal is given based off the change in ETM position. This signal is also the same for a frequency shift.

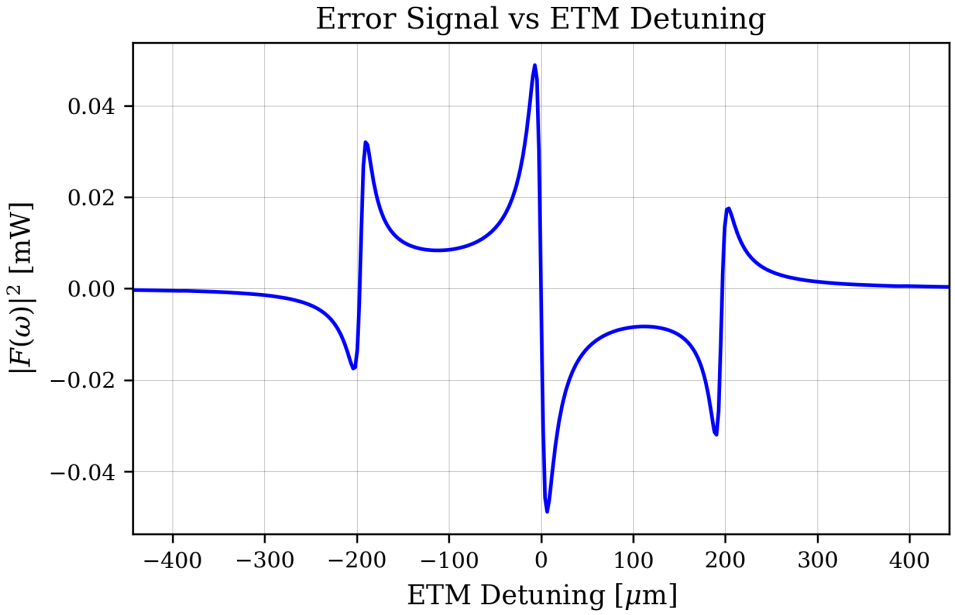

Figure 2.12: *Error Signal given as a function of mirror detuning. This signal can also be given as function of frequency shift, but since we are actuating on the ETM it is useful to show our error signal on the component of the cavity we are actuating on.*

Due to the PDH method, we have transformed our intensity signal to become linear around resonance, which enables it to be actuated on by a feedback control system.

3 Beam Characterization

In order to accurately design the visible light cavity's launch optics, the laser's characteristics must be determined. There are two important characteristics that we determine in this report: the mode purity of the Gaussian laser through the M^2 factor, and the polarization and intensity drift. More information about the laser is given in the parts documentation section.

3.1 M^2 measurements

M^2 measurements serve as a way of testing the Gaussian purity of our 532nm laser. The width of the beam as a function of z can be modeled by equation 3.1. For a perfect Gaussian beam comprised of TEM00, $M^2 = 1$. However, for a beam comprised of higher order modes, $M^2 > 1$. Realistically, a laser beam will not be perfect, and thus we conduct these measurements to determine the TEM00 composition of our 532nm laser beam.

$$\omega^2 = \omega_0^2 + \left(M^2\right)^2 \left(\frac{\lambda}{\pi\omega_0^2}\right)^2 (z - z_0)^2 \tag{3.1}$$

The M^2 factor can be easily measured using a combination of lenses and a beam camera. The principle is measure the width of the beam at many various points in its propagation direction, and then fit the data points to the equation. The 532nm laser beam does not converge/diverge on its own. It stays relatively culminated at a width 1 - 1.5 mm. To obtain the a Gaussian-like converge/diverge pattern in its propagation direction, we use a set of lenses placed successively from the beam. A diagram of the lens configuration can be seen in Figure 3.1 below.

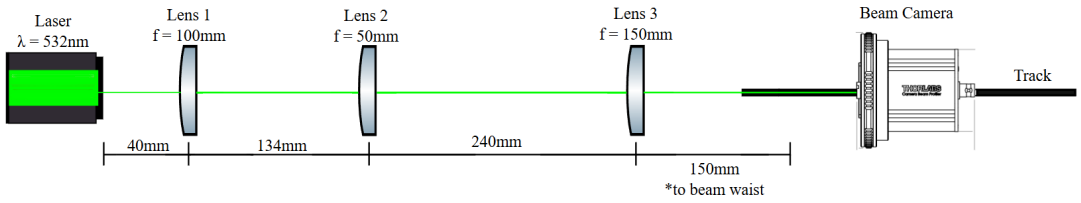

Figure 3.1: *Configuration for taking beam width data. The beam camera is free to slide on the black track for a range of up to 600mm*

The first lens is 100mm in focal length, which gives it is primary Gaussian shape. However, we do not just use one lens to take the M^2 measurements since a single lens focuses the beam down to approximately $50m$, which is too small for the beam camera to resolve. By implementing 50mm and 150mm focal length lenses, we effectively create a telescoping system that makes the beam waist 3x larger.

The data acquisition is rather simple. The Thorlabs beam camera is placed on a track as seen in the diagram. The beam waist should be 150mm from the last lens (considering that is its focal length). With the camera connected to a laptop and the Thorlabs software running, we collect a series of equally spaced data points along the track.

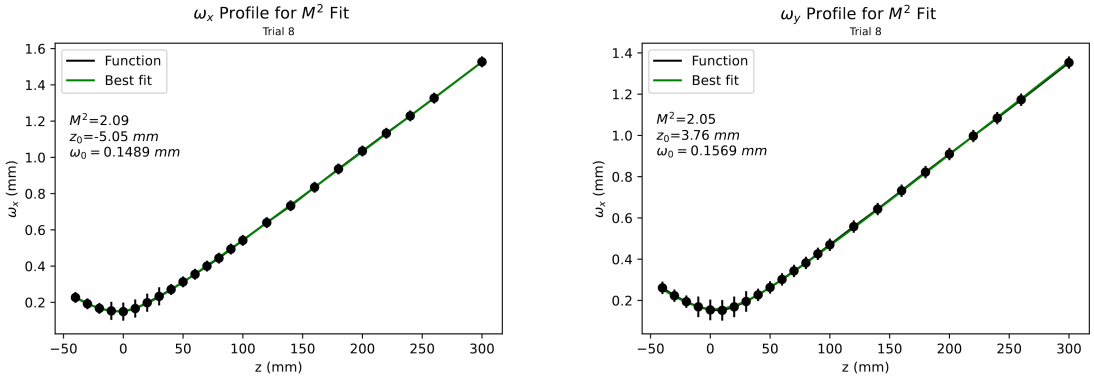

Figure 3.2: *Beam width as a function of z position in both x and y. Both of these plots are fit to find the M^2 value. The data was taken 8 times before it was concluded that these were the final measurements.*

Ideally, data should be taken several mm before the beam waist, at the beam waist, and after the beam waist. Data is also taken past the Rayleigh range. The Thorlabs beam camera measures the beam width in the x and y directions separately. The data can easily be taken in excel or a google spreadsheet and saved as a csv file. The data is then analyzed using a python script to fit the data to equation (3.1). The results of the measurements are shown in Figure 3.2 for the x and y directions.

From the Figure, it is clear that our $M^2 \approx 2$ for both the ω_x and ω_y directions. This indicates that our laser beam is comprised of a significant percentage of higher order modes. Because we have a largely non-Gaussian laser beam, we expect a significant portion of the laser power to be rejected from the cavity due to these Higher order modes.

3.2 Polarization and intensity drift

Another important test to conduct with our laser is how well it maintains its target intensity and how much its polarization axis drifts. Characterizing polarization and intensity drifts is majorly important, as it inevitably tells us how well and how long we are able to maintain resonance. If laser polarization or intensity change too rapidly, then we are likely not be able to hold the cavity on resonance for very long.

In order to distinguish between power fluctuations and polarization drifts, we implement the set up shown in Figure 13. The laser first propagates through a half-wave plate on a rotatable mount. By having the laser propagate through the half-wave plate, we are able

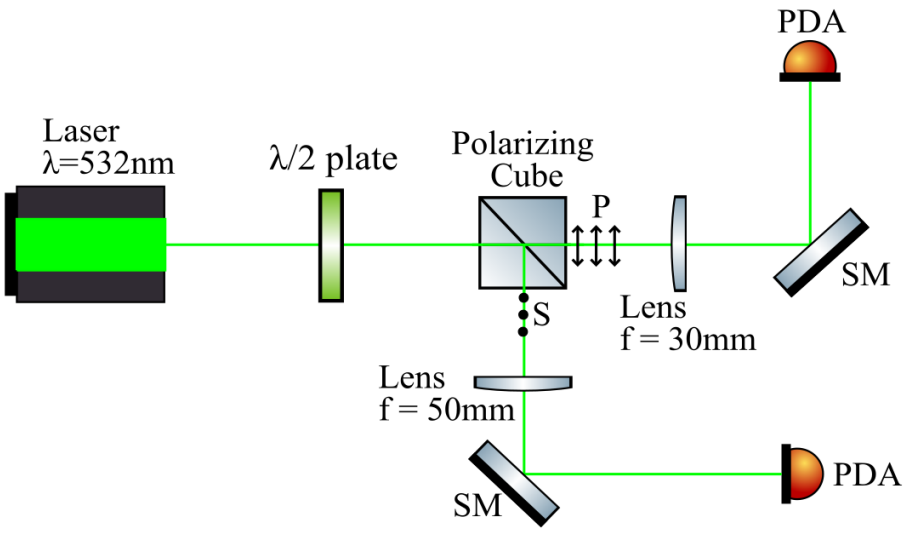

Figure 3.3: *Tabletop set-up to take polarization drift measurements. The horizontal polarization is denoted P-polarization, and the vertical polarization is S-polarization.*

to fine tune the polarization of the laser such that maximum power is transmitted through each direction of the polarizing cube. This also allows us to ensure that there is equivalent power going into both directions.

At the polarizing cube, the beam is split into two directions. The S-polarization is deflected, and the P-polarization is transmitted through. In each direction, the laser is propagated through a lens in order to focus it into a smaller size. The stirring mirrors then guide each laser into photo-detectors.

The photo-detectors convert the raw laser power into a DC voltage signal. The two DC outputs are then sent to a Red Pitaya. The Red-Pitaya has many various functions, but for this analysis, it's most useful functions will be its built-in oscilloscope, and its ability to read and store data values for every given integer of time.

For this analysis, we denote the P-polarization voltage signal S_P and the S polarization voltage signal S_s. Hence, to find S and P polarization powers, we have:

$$\begin{aligned} S_P &= C_P P_P \\ S_S &= C_S P_S \end{aligned} \tag{3.2}$$

Where P_P and P_S are the powers of the relative polarizations, and C_S and C_P are calibration constants allowing us to convert from power in watts to voltage in volts. Before we begin this analysis, these constants are determined by comparing the ratio of Wattage reading on a power meter to the voltage received on the Red-Pitaya's oscilloscope. For these measure-

ments, $C_P = 1.374 \pm 0.0099 \frac{Volt}{Watt}$, and $C_S = 0.947 \pm 0.027 \frac{Volt}{Watt}$

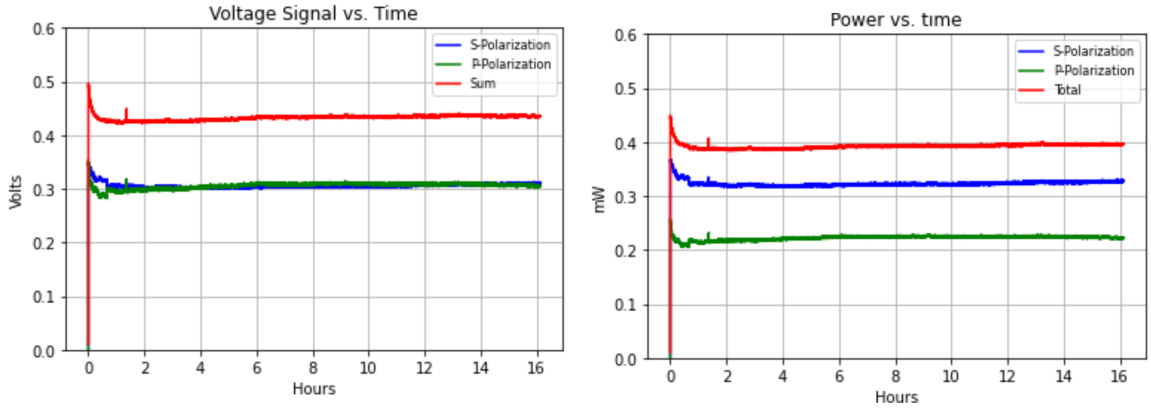

Figure 3.4: *Left: Plot of Red-Pitaya Signal as a function of time. This plot is the raw data values, S_P and S_S from each of the PDA's without calibration. Right: Plot of the power, P_P and P_S when calibration constants are included.*

The Red Pitaya is set to take data every 1.074 seconds. The laser is turned on and left to run for approximately 16 hours. Each of Figure 3.4 plots show the drifts of the laser's power in the S-Polarization and P-Polarization directions. From a rough glance, it seems as though the laser maintains decent stability in both its total power and its polarization angle.

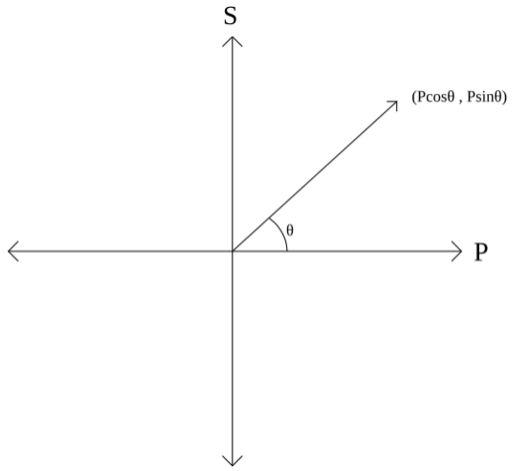

Figure 3.5: *Diagram of S-P polarization. The polarization angle, θ will be defined as the formed by the laser's polarization axis with respect to horizontal.*

To further analyze our laser stability, the relative polarization powers can be broken up into sines and cosines as shown in the diagram above. We end up with:

$$\begin{aligned} P_P &= P\cos(\theta) \\ P_S &= P\sin(\theta) \end{aligned} \tag{3.3}$$

Finally, in order to get the polarization angle θ, we have:

$$\begin{aligned} \frac{S_P}{C_P} &= P\cos(\theta) \\ \frac{S_S}{C_S} &= P\sin(\theta) \end{aligned} \tag{3.4}$$

$$\left(\frac{S_S}{C_S}\frac{C_P}{S_P}\right) = \frac{\sin(\theta)}{\cos(\theta)} = \tan(\theta) \tag{3.5}$$

$$\theta = \tan^{-1}\left(\frac{S_S}{C_S}\frac{C_P}{S_P}\right) \tag{3.6}$$

In which S_S and S_P are acquired through the Red Pitaya's read-in signal.

From here, the total power is able to be easily obtained:

$$P = \sqrt{P_P + P_S}$$

.

From figure 3.6, it is more easily determined the stability of our laser's total power and its polarization angle. For both cases, it is clear that there is marginal fluctuation in the first 1-2 hours. Over longer periods of time, our polarization angle maintains exceptional stability. The total intensity continues to fluctuate throughout nearly the entire 16 hours, yet it is still relatively negligable, which allows us to continue constructing the visible light optical cavity.

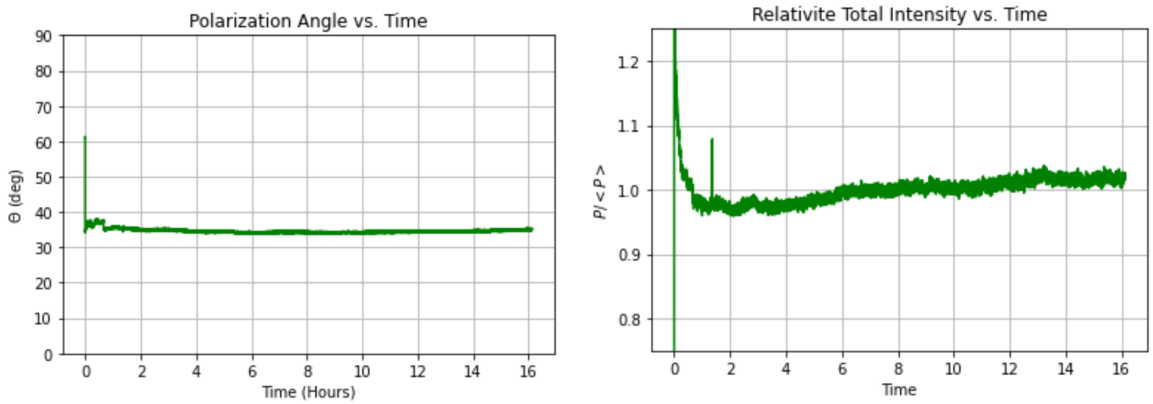

Figure 3.6: *Left: θ in degrees as a function of time. Right: Relative power, $\frac{P}{\langle P \rangle}$*

These polarization measurements not only help us determine how stable our laser power is, but we now know what to expect when the laser is left on for long periods of time, and we are able to adjust accordingly.

4 Installation and Assembly

4.1 Launch Optics

Once all of the modeling for the visible light cavity is completed and the parts have been acquired, physical assembly begins with the launch optics. Figure 4.1 shows the set up for the launch optics. This section will detail the purpose / function for each component.

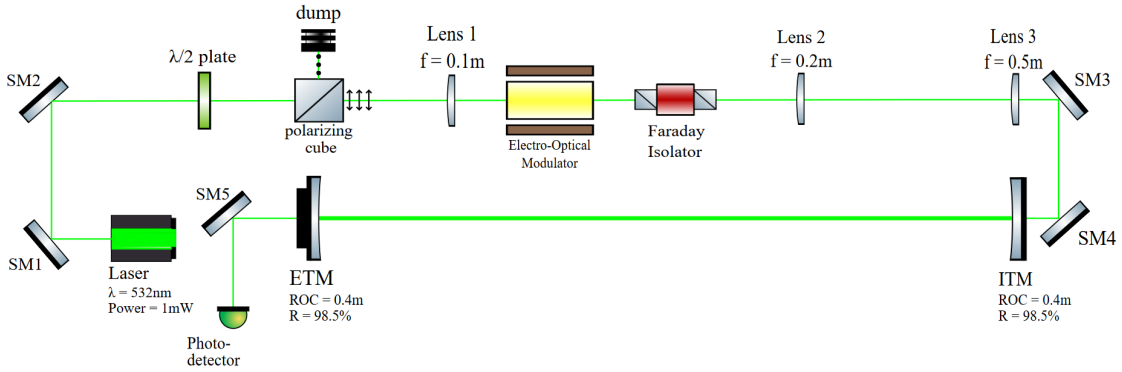

Figure 4.1: *Launch Optics design for Visible Light Cavity. Refer to text for detailed explanation of each component and their set up.*

The laser height is set to 3 inches, and it is propagated through two stirring mirrors (SM1 and SM2). These mirrors are strategically placed right in front of the laser path in order to allow multiple degrees of freedom for adjustment. SM1 is placed very close to the laser allowing for easy tuning capability. Adjusting this mirror will adjust the vertical height and horizontal position of the laser. SM2 is placed not too far away and this will control the horizontal and vertical angle of the laser.

The half-wave plate and polarizing cube is then placed directly after SM2. The polarizing cube deflects vertically polarized light and allows horizontally polarized light through. The half-wave plate is rotationally adjustable, and it rotates the raw field of the beam. We place it prior to the polarizing cube in order to get the maximum power transmission through the cube. The reason we only want a single polarization direction going on from here is because the Faraday isolator will only work optimally if the light entering is at a single polarization.

Lens 1 is placed directly prior to the EOM and Faraday isolator in order to focus the beam down to a size capable of fitting within both the EOM and Faraday isolator ports. Up until now, we have not measured the distance of any of these launch optics to each other, but now the distance becomes measured. The beam waist is approximately 100mm away from Lens 1 and this beam waist occurs within the EOM. We now define the beam waist position as z = 0 and we will measure our optic's distances from here.

The EOM and Faraday isolator are placed in succession in order to start the PDH lock. As

discussed in section 2.4, the EOM will take a portion of the beam's power and modulate it to +/- 20MHz. It is place roughly at z = 0. The Faraday isolator will further polarize the beam into a specific direction, and deflect the reflected beam in order to read its error signal. It is placed roughly at z = 0.1m.

From section 2.1 and 2.3, we already know that the purpose of the mode matching telescope is to transform the beam and its q parameter to match the input q parameter of the cavity. Lens 2 is placed at z = 0.1898m. Lens 3 is placed at z = 0.3284m. The focal lengths are shown in Figure 4.1.

Since we have an ample amount of space between Lens 3 and the ITM (which is placed at z = 0.5497m) we put two more stirring mirrors. These mirrors are crucial for commissioning the cavity by guiding the beam properly into the cavity axis. The second stirring mirror is place only 5cm away from the ITM in order to have optimal adjustment on the ETM without affecting the position too much on the ITM.

The ITM and ETM are placed exactly 0.55mm away from each other. The ETM is placed in a Piezo-Electro Mount which has adjustment knobs connected to a PZT actuator (see section 4.3). This enables the ETM to be adjusted from the PDH lock. The laser beam then propagates to a photo-detector for readout purposes.

The full launch optics set up is shown in Figure 4.2.

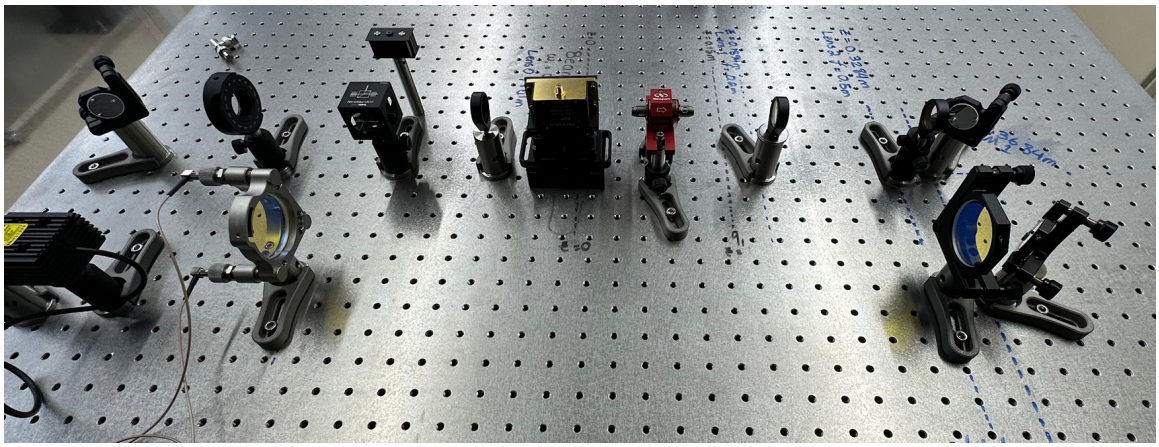

Figure 4.2: *Lab photograph of Visible Light Cavity Launch Optics*

4.2 Commissioning the Cavity Axis

It is nearly impossible to get the perfect mode matching and stable laser transmission on an initial installation. There is a careful procedure in placing the optics to create a perfect cavity axis and align the laser to it as well as possible.

In practice, after placing the two stirring mirrors after the Faraday isolator, the photo-detector (and SM5) is placed immediately afterwards. The laser is turned on, and the photo-detector is connected to an oscilloscope. The stirring mirrors are then adjusted to place maximum power into the photo-detector. This power can be measured via the oscilloscope to find the optimal stirring mirror adjustment.

Then the ETM is placed in its position 0.999m away from the beam waist. The ETM position and surface is manually adjusted so that the beam is incident squarely in the center of the mirror and at a normal incidence. An easy way to check the normal incidence is the reflection off of the ETM surface. Upon normal incidence the reflected beam propagates directly back in the direction it comes in. This means that the reflected beam propagates back into the Faraday isolator and can be read in the deflection port. A power meter is placed in the deflection port of the Faraday isolator and maximized by adjusting the pitch and yaw of the ETM.

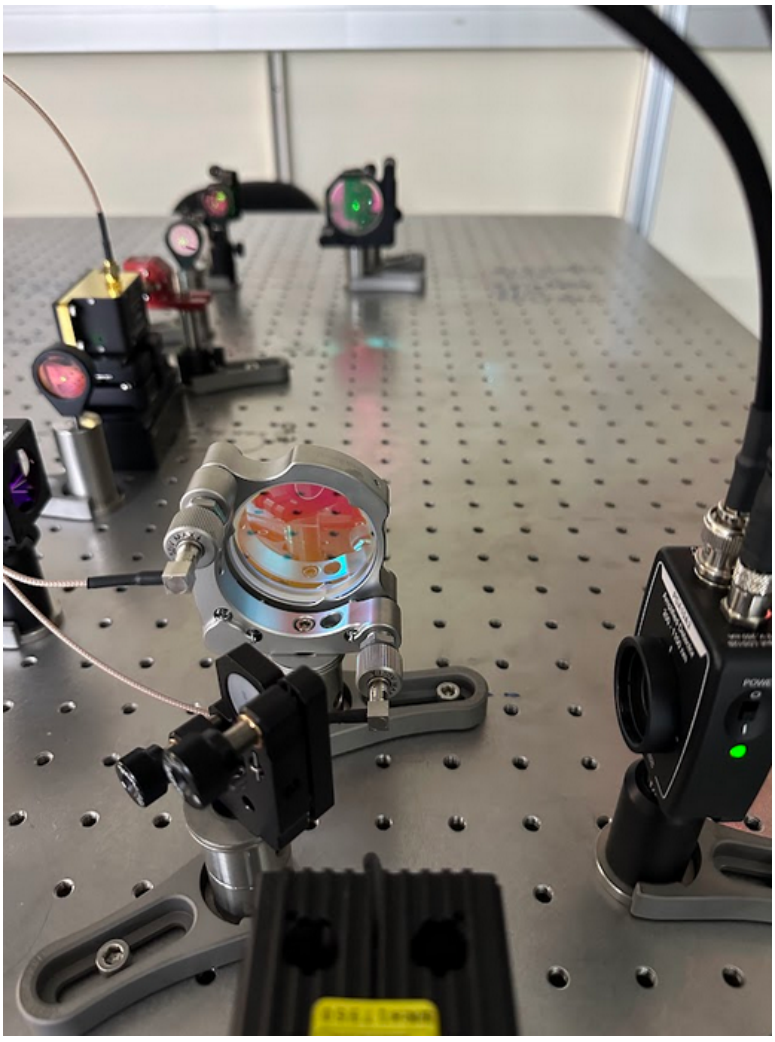

Figure 4.3: *ITM transmission to photo-detector*

Once the beam is perfectly aligned to the photo-detector and ETM, the ITM is then placed

0.549m away from z = 0. The ITM is then manually adjusted to have the laser hit squarely on its center and at a normal angle. Once the ITM is in place, there are likely a few "ghost beams" on the ETM. These are the reflections from the beam propagating back and forth within the non-perfect cavity. The existence of ghost beams within the cavity mean that the surface of the ITM is not perfectly aligned normally with the surface of the ETM (thus the cavity axis is not perfectly aligned). In order to perfectly align the cavity axis, the ITM tuning knobs are adjusted to algin all of these ghost beams onto one spot on the ETM. This ensures that the beam propagating back and forth within the cavity travels the exact same path.

Finally, the transmitted light of the beam is read on the photo-detector and fed to an oscilloscope. Any voltage signal means that there is transmitted power and the cavity is resonating to some degree. This set up is shown in Figure 4.3

4.3 PDH Lock

Finally, we incorporate the PDH lock in order to maintain resonance. We refer to information given in section 2.4 to describe each feedback control component of Figure 4.4.

The EOM is being driven at +/- 20MHz by the signal generator. This same signal generator is also driving the mixer, ensuring that the modulation frequency is equivalent in both the EOM and the mixer. As the beam goes into the cavity and returns back into the Faraday Isolator, the beam is deflected into a Stirring mirror and photo-detector. The SM and lens combination is to ensure that the full beam spot is focused and aimed perfectly onto the photo-detector.

The photo-detector converts the signal (which contains the error and beat note) into a voltage signal. Since we anticipate already having a large amount of power rejected from our cavity, we incorporate a Bias tee to discard the DC offset we have in the reflection. The only signal left is an AC signal going into the mixer.

Our PDH lock is an analog lock system. The frequency mixer simply multiplies its inputs from the Bias Tee and the Signal Generator, and outputs the error signal to the SR560. The SR560 acts as both the low pass filter and the gain amplifier. It allows only low frequency DC signal to pass through, which is amplified.

The output from the SR560 is then sent into a PDu150, which controls the PZT's on the ETM. The error signal determines what actuation is needed on the ETM.

As of this writing, the Lock of the Visible Light Cavity is Yet to be achieved. We are able to attain a 20% mode matching without lock. This was done with the commissioning process described in the previous section. The mode matching is done without a lock. However, in future work, it will likely take minimal effort to set up this configuration and achieve a lock.

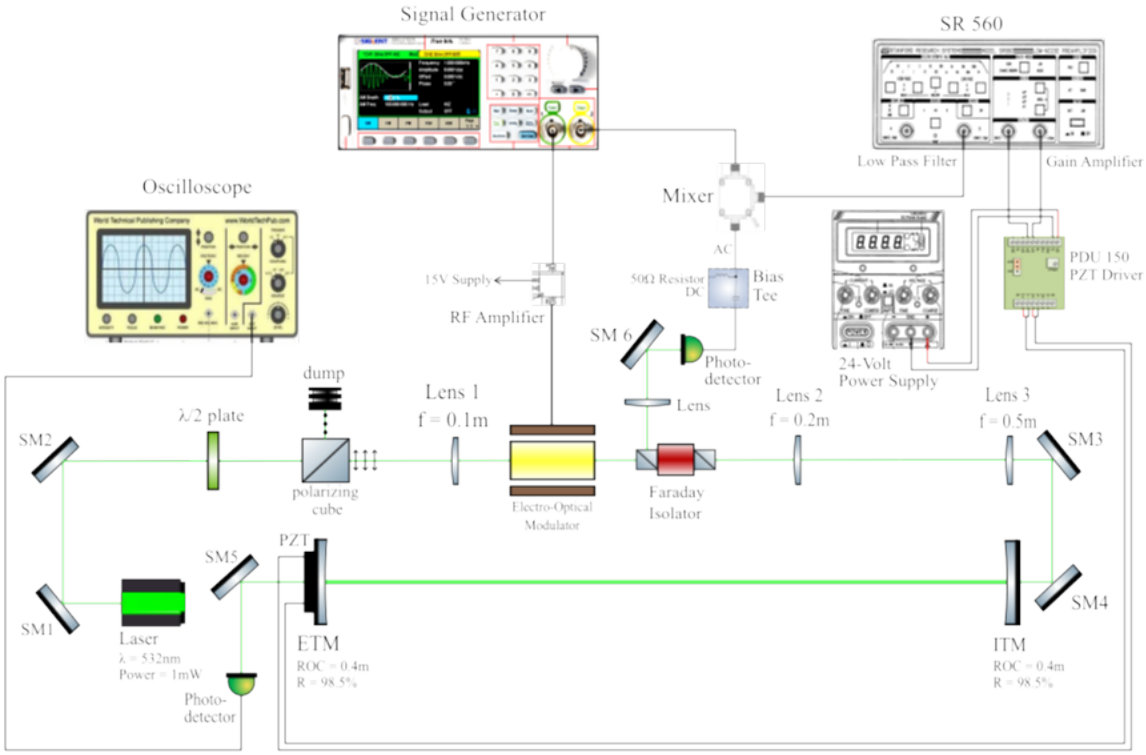

Figure 4.4: *The full design of the visible light optical cavity. Prior to the cavity is a chain of launch optics to prepare the beam to enter the cavity. The cavity is stabilized by a feedback control system. These components will all be explained in the following sections*

References

[1] Charlotte Bond, Daniel Brown, Kenneth Strain, Andreas Freise. *Interferometer Techniques for Gravitational-Wave Detection*. https://arxiv.org/abs/0909.3661 (2015).

[2] H. Kogelnik and T. Li. *Laser Beams and Resonators* https://opg.optica.org/ao/fulltext.cfm?uri=ao-5-10-1550&id=14408 (1966)

[3] Eric D. Black *An introduction to Pound–Drever–Hall laser frequency stabilization* American Physics Journal. DOI: 10.1119/1.1286663. (2000)

[4] *Frequency domain INterferomEter Simulation SoftwarE* http://www.gwoptics.org/finesse

[5] *Finesse Software* https://finesse.ifosim.org/

[6] Rudiger Paschotta, *Finesse* https://www.rp-photonics.com/finesse.html